

Differential associations between scale-free neural dynamics and different levels of cognitive ability

Leisi Pei¹  | Xinlin Zhou²  | Frederick K. S. Leung¹  | Guang Ouyang¹ 

¹Faculty of Education, The University of Hong Kong, Hong Kong, China

²State Key Laboratory of Cognitive Neuroscience and Learning, IDG/McGovern Institute for Brain Research, Beijing Normal University, Beijing, China

Correspondence

Guang Ouyang, Faculty of Education, The University of Hong Kong, Hong Kong, China.

Email: ouyangg@hku.hk

Funding information

Hong Kong Research Grant Council, Grant/Award Number: 17609321 and 27603818

Abstract

As indicators of cognitive function, scale-free neural dynamics are gaining increasing attention in cognitive neuroscience. Although the functional relevance of scale-free dynamics has been extensively reported, one fundamental question about its association with cognitive ability remains unanswered: is the association universal across a wide spectrum of cognitive abilities or confined to specific domains? Based on dual-process theory, we designed two categories of tasks to analyze two types of cognitive processes—automatic and controlled—and examined their associations with scale-free neural dynamics characterized from resting-state electroencephalography (EEG) recordings obtained from a large sample of human adults ($N = 102$). Our results showed that resting-state scale-free neural dynamics did not predict individuals' behavioral performance in tasks that primarily engaged the automatic process but did so in tasks that primarily engaged the controlled process. In addition, by fitting the scale-free parameters separately in different frequency bands, we found that the cognitive association of scale-free dynamics was more strongly manifested in higher-band EEG spectrum. Our findings indicate that resting-state scale-free dynamics are not universal neural indicators for all cognitive abilities but are mainly associated with high-level cognition that entails controlled processes. This finding is compatible with the widely claimed role of scale-free dynamics in reflecting properties of complex dynamic systems.

KEYWORDS

$1/f$, automatic and controlled process, cognitive ability, dual-process theory, resting-state EEG, scale-free dynamics

1 | INTRODUCTION

1.1 | Scale-free neural dynamics and their functional and cognitive associations

Scale-free dynamics are ubiquitous in nature and are found at multiple neural activity levels (Allegrini et al., 2009;

Cocchi et al., 2017; He, 2011, 2014). They refer to aperiodic neural activity with self-similarity across temporal scales and are manifested as a $1/f$ -like distribution in the power spectrum (He, 2014). By definition, scale-free dynamics reflect a stationary, rather than transient, process, the characterization of which is based on (relatively) long-term statistical features. From a dynamic system point of

This is an open access article under the terms of the [Creative Commons Attribution](https://creativecommons.org/licenses/by/4.0/) License, which permits use, distribution and reproduction in any medium, provided the original work is properly cited.

© 2023 The Authors. *Psychophysiology* published by Wiley Periodicals LLC on behalf of Society for Psychophysiological Research.

view, scale-freeness is a defining feature of self-sustaining nonlinear dynamic systems that exhibit criticality phenomena (Cocchi et al., 2017), which has been proposed to underpin the functional optimality of neural systems in various aspects, including dynamic flexibility (Kinouchi & Copelli, 2006) and computational capacity (Beggs, 2008; Cocchi et al., 2017; Shew & Plenz, 2012), although this notion is still under debate (Beggs & Timme, 2012). The scale-freeness reflects the property of a complex nonlinear system that displays flexibility in transitioning between various dynamic patterns during its spontaneous activity, leading to higher ability in coping with variability and uncertainty in external inputs (Cocchi et al., 2017). When (self-)configured into optimal states with respect to a specific function, neural systems can display these optimal states already in their ongoing spontaneous dynamic activity without being engaged in a task that performs the functions (Cocchi et al., 2017). Therefore, the scale-freeness of resting-state neural activity would be able to predict functional performance in task.

The functional relevance of scale-free dynamics has been increasingly recognized in recent decades (He, 2014; He et al., 2010; Voytek et al., 2015). This has led to a burgeoning of studies, particularly in recent years, reporting strong correlations between parameters of scale-free dynamics and various neurocognitive and physiological factors, such as arousal state (Colombo et al., 2019; Gifani et al., 2007; Lendner et al., 2020), sensory deprivation (Weber et al., 2020), development and aging (Churchill et al., 2016; Dave et al., 2018; McSweeney et al., 2021; Merkin et al., 2023; Thuwal et al., 2021; Voytek et al., 2015), mental disorders (Ostlund et al., 2021), task effortfulness (Churchill et al., 2016; Kardan et al., 2020; Kasagi et al., 2017), and cognitive ability (Bongers et al., 2020; Huang et al., 2016; Immink et al., 2021; Kasagi et al., 2017; Kolvoort et al., 2020; Ouyang et al., 2020). However, it is important to note that the use of the term “scale-free” and the underlying concepts are still ambiguous in the field. This is reflected in different terms used to describe similar dynamic features such as $1/f$ (Voytek et al., 2015), aperiodic component (Donoghue et al., 2020; McSweeney et al., 2021), fractal structure or fractal scaling (Gifani et al., 2007; Pereda et al., 1998; Wen & Liu, 2016). Some of these previous literatures deliberately chose terms to avoid conceptual ambiguity, whereas others used them interchangeably. In the present article, we will use the term of scale-free and $1/f$ interchangeably to refer to the dynamic feature of the downward-going, straight-line-like spectrum pattern in the log–log space.

Among the past research studying the functional association of scale-free neural dynamics, the association with cognitive ability measured through different cognitive tasks is a major domain. The cognitive performance or abilities

associated with scale-free parameters in numerous studies have covered multiple functional domains, including cognitive control (Clements et al., 2021), attention (Waschke et al., 2021; Zhang et al., 2021), working memory (Kardan et al., 2020), face and object recognition (Kasagi et al., 2017; Ouyang et al., 2020), motor performance (Immink et al., 2021), academic learning (Bongers et al., 2020; Cross et al., 2022), and sense of self (Huang et al., 2016).

The present work is aimed at examining the association between the estimated parameters characterizing scale-free features in neural activity and human cognitive abilities. Based on the abovementioned extensively reported associations, scale-free neural dynamics are undeniably reflective of the functionality of the cognitive system. However, an important question arises from the multitude of findings that remain to be answered: are scale-free dynamics universally associated with a wide spectrum of cognitive abilities or are they specific to a certain level or type of cognitive process?

1.2 | Fine-graining the association of scale-free dynamics with cognitive abilities over different levels of cognition

It is important to answer the question above to delineate the functional role of scale-free dynamics in human cognition and to support studies determining the underlying neural mechanisms. If the association is universal, scale-free dynamics would manifest the domain-general information-processing capacity required for a great variety of cognitive activities; this may explain the reported associations in a wide variety of tasks (Duncan, 2010; Fedorenko, 2014; Gilmore & Cragg, 2018). In contrast, human cognition is a complex system comprising hierarchical levels of inter-woven cognitive processes (Craik & Lockhart, 1972; Miller & Wallis, 2009); therefore, scale-free dynamics are unlikely to be universally predictive of cognitive processing at all levels. This question can be addressed by administering various cognitive tasks while manipulating a cognitive factor in a well-controlled way within the same study (preferably based on a large sample size) and examining how task performance is differentially associated with the scale-free dynamics measured in the resting state. The cognitive factor to be manipulated should be fundamental and theoretically more likely to differentiate different neural cognitive systems, such as different levels, complexities, or demands in information processing. Previous studies have not directly addressed this point by distinguishing the scale-free dynamics–cognition associations among different cognitive systems; however, those studies have provided interesting and useful aggregate patterns that can be used to foster new

hypotheses. For example, the associations reported in most studies have been based on tasks that mainly involve strenuous cognitive control (Bongers et al., 2020; Immink et al., 2021; Kardan et al., 2020; Ouyang et al., 2020; Voytek et al., 2015). Accordingly, in this study, we formulated the following research questions and the corresponding hypotheses.

First, we questioned whether scale-free dynamics are differentially associated with cognitive abilities at different levels of cognition. How complex human cognition is structured is a major question in cognitive science (James, 1890; Nelson et al., 2015). In a generic sense, different levels of cognitive processes differ in complexity (e.g., processing a single color vs. evaluating fine arts). Dual-process theory, which is a well-established cognitive theory supported by several theoretical and empirical studies (for a review, see Evans & Stanovich, 2013; Milli et al., 2021), clearly proposes two distinct types of cognitive processes: automatic and controlled (Schneider & Shiffrin, 1977). The primary distinction between these two types lies in the required amount of working memory resources (Evans, 2011). Automatic processes are characterized by (1) minimal access to working memory resources and the recruitment of few top-down control processes, (2) having a fixed routine, and (3) being generally fast and effortless. In contrast, controlled processes are characterized by (1) a strong reliance on working memory resources and cognitive control processes, (2) flexibility to cope with novel situations, and (3) being generally slow and strenuous. Both of these processes interplay under a hierarchical human cognitive system wherein automatic processes play at a low level and controlled processes play at a high level (Evans, 2011; Evans & Stanovich, 2013; Schneider & Chein, 2003).

The distinction between these two processes based on dual-process theory forms a foundation for our hypothesis regarding the first research question: the two types of cognitive processes may be differentially associated with resting-state scale-free neural dynamics. First, as mentioned above, the cognitive associations of scale-free dynamics reported in most previous studies have been based on tasks involving controlled processes (Bongers et al., 2020; Immink et al., 2021; Kardan et al., 2020; Ouyang et al., 2020; Voytek et al., 2015). Second, from a theoretical perspective, scale-free dynamics are a defining characteristic of complex systems that behave flexibly and unpredictably (Cavanna et al., 2018; Cocchi et al., 2017; Kelso, 2012). Flexibility refers to the ability of a dynamic system to intermittently and actively escape from an attractor and shift to another (Kelso, 2012), thereby forming a rich set of activity patterns. Compared with automatic processes that are fixed and routine, this characteristic is more compatible with high-level controlled processes

that are complex and flexible. Taken together, we concretize our hypothesis about the first research question as follows: scale-free neural dynamics should be associated with cognitive performance in high-level tasks that involve high-level controlled processes to a greater extent than with cognitive performance in low-level tasks that mainly involve low-level automatic processes.

1.3 | Characterization of scale-free neural dynamics

As a neural indicator of properties of the underlying functional cognitive system, scale-free dynamics have been commonly characterized from the resting state (Colombo et al., 2019; Immink et al., 2021; Kolvoort et al., 2020; Ostlund et al., 2021; Ouyang et al., 2020) based on the assumption that spontaneous (task-free) neural dynamics predict task-measured behavioral performance (Anderson & Perone, 2018; Cole et al., 2016). The in-task measurement of scale-free dynamics has also been applied in a conceptually sensible way, for example, studying how scale-free dynamics change as a function of task demand (Churchill et al., 2016). Regardless of the data source, the scale-free dynamics should be characterized using data accumulated over a long period to achieve adequate statistical reliability.

Despite the existence of well-established methods for characterizing scale-free dynamics, there is still an open issue in terms of parameterization, which is rooted in the reality of the neural activity feature. In fact, the power spectrum of neural physiological signals in the log–log space does not strictly follow a single straight line. Rather, the $1/f$ -like pattern is usually confined to specific frequency ranges or separated into multiple segments with different slopes. This issue has been commonly reported in the literature, as evidenced by previous methods that used various bands for estimating scale-free dynamics (Chaudhuri et al., 2017; Donoghue et al., 2020; He, 2014; Lendner et al., 2020). In light of this issue of reality-theory discrepancy, it is reasonable to hypothesize that the statistical results regarding the cognitive association of scale-free parameters may depend on how the non-straightness of $1/f$ -like pattern in the log–log space is treated in the model fitting procedures. Therefore, in this study, we examined the results over different variations of data-fitting procedures.

1.4 | The present study

To address the research questions outlined above, we designed a series of cognitive tasks to measure five cognitive abilities at different levels and correlated them with

the resting-state neural dynamics of 102 adult participants measured from their electroencephalography (EEG) recordings. We compared the association with scale-free dynamics across cognitive abilities at different levels. In brief, we included two low-level tasks that mainly involved automatic processes and three high-level tasks that involved controlled processes. The associations between the cognitive abilities and resting-state scale-free dynamics were then examined from different fitting procedures including (1) fitting at different frequency ranges: a low band of 1–25 Hz and a high band of 26–90 Hz and (2) fitting the aperiodic component with a bending parameter characterizing the curvature. The consistency of the result pattern was examined, and their implications were discussed.

2 | METHOD

2.1 | Experimental design

2.1.1 | Participants

A total of 102 right-handed young adults with university education or above were included in this study. All the participants (mean age = 25.3 ± 3.8 years; 50 men) were native Chinese speakers from mainland China, reported normal or corrected-to-normal vision, and had no history of mental diseases. The experimental protocol was approved by the Human Research Ethics Committee of the University of Hong Kong. Informed consent was obtained from all of the participants prior to the start of the experiment.

2.1.2 | Experimental tasks

All experiments were conducted in a sound-attenuated room. The participants were seated comfortably in front of a presentation display and instructed to complete a series of cognitive tasks with their EEG signals being recorded. EEG recordings from a resting-state task and behavioral data from the five cognitive tasks related to the present study were included for analysis.

Resting-state task with EEG recordings

The resting-state task included an eyes-open and an eyes-closed session, each of which lasted for 60 s. In the eyes-open session, the participants were instructed to sit still and relax with their eyes open (natural eye blinks were allowed); in the eyes-closed session, the participants were required to keep their eyes closed throughout the session. During the task, the participants wore an elastic EEG cap

(actiCAP, Brain Products), with the electrodes placed following the international 10–20 system (Pivik et al., 1993). Continuous EEG signals were recorded using a 32-channel BrainAmp DC amplifier (Brain Products), online referenced to the ground electrode of the amplifier, digitalized at 1000 Hz, and stored using BrainVision PyCoder.

Although both the eyes-open and eyes-closed sessions were included in the resting-state task, the characterization of scale-free dynamics in this study was performed using the EEG data from the eyes-open session only because all the cognitive tasks included in the present study were conducted in the natural eyes-open state (see below). The eyes-closed session served to validate the correctness of the EEG data based on the well-known Berger effect (Barry et al., 2007; Bazanova & Vernon, 2014), which specifies that the spectral power in the alpha band (8–12 Hz) is significantly higher in the eyes-closed state than in the eyes-open state.

Cognitive tasks with behavioral responses

After the resting-state task, the participants were instructed to complete five cognitive tasks (Figure 1), including a (1) pointing-arrow simple reaction time task (P-SRT), (2) moving-arrow simple reaction time task (M-SRT), (3) task-switching (TS) task, (4) visuospatial working memory task (VSWM), and (5) mental calculation task (MC). P-SRT, M-SRT, and TS were performed first and the order of them were counterbalanced across all participants. VSWM and MC were performed as the fourth and fifth task, respectively. The details of the five cognitive tasks are provided below.

Task #1: Pointing-arrow simple reaction time task. This was a low-level task that was assumed to primarily involve an automatic sensorimotor process and minimal controlled process because the participants only needed to provide motor responses based on the pointing direction of arrows, which is simple and easily recognizable. In each trial, a set of identical arrows pointing to one of four directions (up, down, left, or right) were constantly moving to one of four directions (up, down, left, or right) on the screen. The pointing direction of the arrows differed from their moving direction in each trial; moreover, the pointing directions of the arrows were different between adjacent trials. The participants were instructed to respond by pressing the arrow key corresponding to the pointing direction of the arrows while ignoring any other information (e.g., moving direction). P-SRT comprised 30 formal trials.

Certain design principles were adopted in P-SRT. First, to better distinguish the pointing direction, the arrows were designed with one head and two tails (Figure 1a). The head and tails were dyed in different colors (green and

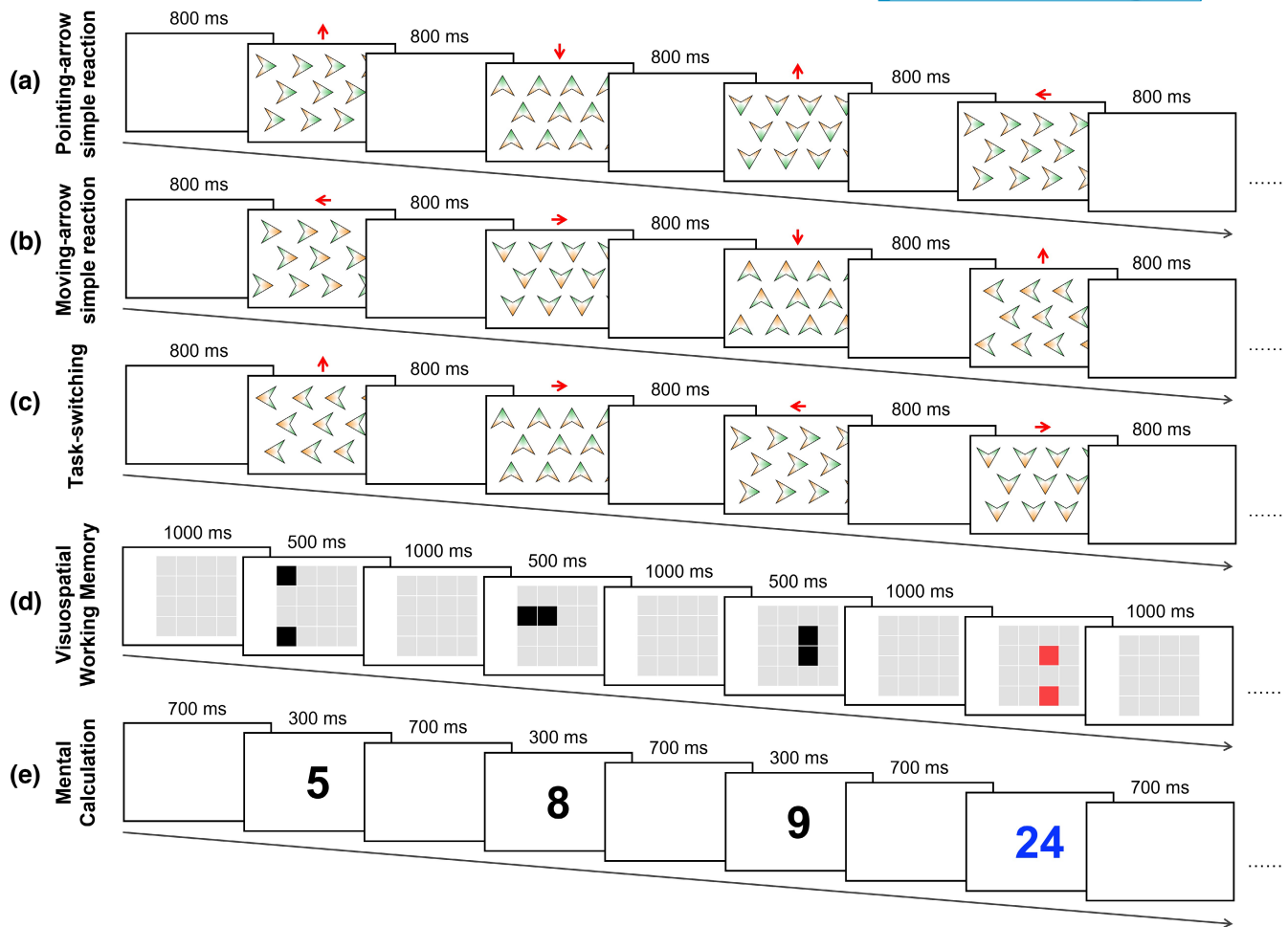


FIGURE 1 Illustration of the five cognitive tasks. (a–c) Four example trials for the pointing-arrow simple reaction time task (P-SRT), moving-arrow simple reaction time task (M-SRT), and task-switching task (TS). In TS, the color scheme with the green-headed arrow cues the P-SRT condition, whereas the color scheme with the orange-headed arrow cues the M-SRT condition. The red arrows above (not shown in the experiment) denote the moving direction of the arrows on the screen. The set of identical arrows keeps moving towards the moving direction on the screen until the participant responds. (d–e) An example trial from the visuospatial working memory task and mental calculation task.

orange), and the dyed areas for the two colors were equal. Second, two opposite color schemes were used for the arrows: one was a green head with orange tails (hereafter, green-headed arrows) and the other was an orange head with green tails (hereafter, orange-headed arrows). For each participant, a specific color scheme (one of the two) was assigned for the arrows in P-SRT. The other scheme was automatically assigned to the arrows in M-SRT (see below). The color scheme in P-SRT or M-SRT was irrelevant within these two separate tasks but relevant to the entire task series (please see below for an explanation).

Task #2: Moving-arrow simple reaction time task. Similar to P-SRT, this task was a low-level sensorimotor-dominant task. The setting in this task was identical to that in P-SRT, except that the response was judged according to the moving direction of the arrows and the color scheme was

different from that in P-SRT. Again, the moving direction of the arrows was different from their pointing direction in each single trial as well as between adjacent trials. M-SRT also comprised 30 formal trials. P-SRT and M-SRT were both simple tasks that are based on a very simple rule and do not involve a component that may elicit cognitive control (such as rule switching and stimulus ambiguity). Thus, they were assumed to primarily capture automatic processes.

Task #3: Task-switching task. Switching between different task conditions based on cues predominantly entails controlled processes and is commonly used to measure cognitive flexibility (Koch et al., 2018). This task served as a high-level cognitive task for assessing the participants' cognitive switching abilities, and was customized based on an effective TS online game (Steyvers et al., 2019).

In this task, the participants were instructed to switch between P-SRT and M-SRT based on the different color schemes (note that the color scheme becomes relevant at this point) assigned to the arrows. Specifically, the arrows in each trial were either green-headed or orange-headed as separately shown in P-SRT and M-SRT. The two types of arrows (i.e., the two color schemes) were pseudo-randomly distributed across the trials (see below for the detailed randomization design), and the participants were instructed to respond according to the specific color scheme in each trial as if they were frequently switching between P-SRT and M-SRT. The TS task comprised 60 formal trials intermixed with 30 trials for the pointing condition and 30 trials for the moving condition. To avoid any expectancy effects, a switch between the two conditions was made after one or two trials. The 60 trials could be further categorized into repetition trials, which cue the same condition as the previous trial and switching trials which cue a different condition from the previous trial. A reference trial (random in cueing the two tasks) was performed before the first formal trial to categorize the first formal trial but was excluded from analysis.

Before performing the formal P-SRT, M-SRT, and TS, a practice session was arranged to ensure that the participants were familiar with the task instructions. Specifically, the participants were taught when to respond to the pointing or the moving direction of the arrows according to the color schemes. The participants underwent three trials (containing both schemes) to demonstrate their understanding of the tasks. Then, the formal versions of the three tasks were conducted in sequence. The order of P-SRT, M-SRT and TS and the mapping between the task conditions and color schemes were both counterbalanced across all participants.

Task #4: Visuospatial working memory. This was a high-level task that aimed to measure the ability to retain visuospatial information in working memory over a short period. The task was adapted from a visual delayed match-to-sample task (Ma et al., 2017). For each trial, a light-gray 4×4 grid was displayed at the center of the screen throughout the trial (see Figure 1d the leftmost frame). One second after the trial starts, two black squares appear on two random grid cells for 500 ms. After another second, two black squares appear on another two random grid cells for 500 ms. Again, after another second, two black squares appear on yet another two random grid cells for 500 ms (Figure 1d). One second after that, two red squares were shown on the grid until the participants respond. The participants need to memorize the locations of the six black squares and judge whether the two red squares are at the locations of the previous six black squares by pressing the left or right Ctrl key. The mappings between the two

Ctrl keys and their indications for matched/unmatched were counterbalanced across all participants. In each trial, only the following two options were possible for the two red squares: (1) matched trial: both the two red squares shown in the last frame were shown in the positions of the previous six black squares, but each red square was from a different frame, and (2) unmatched trial: only one of the red squares overlapped with one of the six black squares. This task comprised 30 formal trials. Before the task, the participants underwent three practice trials to familiarize themselves with the task instructions.

Task #5: Mental calculation. This was also a high-level cognitive task (Gruber et al., 2001). In each trial, three single-digit numbers colored in black were displayed one by one at the center of the screen. Each number was presented for 300ms, followed by a 700-ms blank. Then, a two-digit number colored in blue was displayed and maintained until the participants responded. The participants were instructed to (1) memorize the first number when it appeared, (2) add the first two numbers when the second number showed up and memorize the sum, (3) add the sum of the first two numbers to the third number when the third number was displayed and memorize the total sum, (4) compare the total sum of the three numbers with a finally presented number (shown in blue), and (5) report the correctness of the sum by pressing either the left or right Ctrl key. The mappings between the two Ctrl keys and their indications for the correct/incorrect answers were counterbalanced across all participants. In each trial, the three single-digit numbers were selected such that the carry operation was needed when calculating the sum of the first and second numbers and when adding the sum of the first two numbers to the third number. This task also comprised 30 formal trials. Before the task, participants underwent three practice trials to familiarize themselves with the task instructions.

In all of the cognitive tasks described above, the participants were instructed to respond as accurately and quickly as possible for each trial. The reaction time (RT) and response correctness of each trial were recorded for performance evaluation.

2.2 | Data analysis

2.2.1 | EEG pre-processing

MATLAB (MathWorks, R2021a) and EEGLAB toolbox (Delorme & Makeig, 2004) were used for preprocessing and analyzing the resting-state EEG recordings. The following pre-processing procedures were conducted for each participant: (1) the EEG data segment

containing the resting-state task (2 min in total) was first epoched based on task markers; (2) the extracted EEG data segment was then down-sampled to 250 Hz and filtered using an EEGLAB in-built high-pass FIR filter (zero-phase, non-causal, filter order: 827 data points, cut-off frequency: 0.5 Hz) at 1 Hz; (3) the average re-reference was applied after interpolating the EEG signals for bad channels (with variance >4 median absolute deviations across all electrodes); (4) the independent component analysis method and MARA toolbox (Winkler et al., 2011) were used on the complete EEG data segment to isolate and automatically eliminate artifact components. The default cut-off probability set in MARA was 0.5, and the average number of artifact components rejected by MARA was 17.4 ± 4.3 .

2.2.2 | EEG spectrum analysis

The frequency spectra were obtained by applying the discrete fast Fourier transform (MATLAB R2021a) to the pre-processed EEG time series segment by segment (each segment was 1-s long). This process was conducted on each electrode and the eyes-open and eyes-closed conditions separately. To remove the AC current at 50 Hz, the spectral amplitude at 50 Hz was replaced by the average value of the amplitudes at 49 and 51 Hz. To generate three indicators for building a latent variable for structural equation modeling (see below), we calculated three average spectra, each from one third of the data (i.e., 20 of 60 segments).

2.2.3 | Parameterization of scale-free dynamics

Scale-free dynamics appear as a $1/f$ -like distribution when converted to frequency power spectra. The terms “ $1/f$ ” or “ $1/f$ -like” are convenient descriptors of the feature that power decreases linearly as a function of frequency in the log–log space; it is important to note that these terms do not, in any way, indicate that it is strictly $1/f$. Because of the straight line pattern (Donoghue et al., 2020; Grigolini et al., 2009; He, 2014; He et al., 2010), the *slope* and *offset* of the straight line in the log–log space are the two defining parameters characterizing the pattern. Despite the theoretical description of the characteristics of scale-free dynamics, multiple methods have been developed to estimate the two parameters, including simple linear regression (Clements et al., 2021; Dave et al., 2018; Huang et al., 2016; Kasagi et al., 2017; Lendner et al., 2020; Voytek et al., 2015), Hurst exponent (Churchill et al., 2016; Kardan

et al., 2020), irregular resampling auto-spectral analysis (Bongers et al., 2020; Cross et al., 2022; Immink et al., 2021; Kolvoort et al., 2020; Weber et al., 2020; Wen & Liu, 2016; Zhang et al., 2021), and fitting oscillations and one-over- f (FOOOF; Donoghue et al., 2020; McSweeney et al., 2021; Ostlund et al., 2021; Thuwal et al., 2021). FOOOF appears to be the most widely used among the methods.

The parameterization of scale-free dynamics in this study was conducted using FOOOF. FOOOF is a model-driven approach that decomposes the spectrum into oscillatory components and scale-free dynamics (i.e., the $1/f$ component; Donoghue et al., 2020). In general, FOOOF models the spectrum as the summation of an aperiodic component that captures the $1/f$ -like pattern in the log–log space and multiple oscillation components that capture the discrete peaks in the spectrum (e.g., alpha peak). Given the non-straightness of the spectral curve in the log–log space as shown in previous studies (Colombo et al., 2019; Lendner et al., 2020), we applied FOOOF in different ways to explore how the cognitive association of extracted scale-free dynamics changes across different settings. The performance of fit by FOOOF measured by R^2 will be reported.

The first treatment is that we split the whole frequency range into two bands separated at 25 Hz and the parameters (i.e., exponent and offset) of the $1/f$ component were separately estimated from each band (i.e., 1–25 and 26–90 Hz). Although the split treatment is at odds with the theoretical definition of scale-freeness, we conducted this analysis to cope with the reality of the data feature and to reveal whether the $1/f$ parameters estimated from the different frequency bands contributed differently to the cognitive association of scale-free dynamics. More discussion about this issue is provided in the Discussion section. We heuristically selected 25 Hz as the split point in this study based on the following considerations: (1) there was a visually discernible inflection point at approximately 25 Hz in our grand average spectra curve (Figure 2a); (2) the $1/f$ component should be fitted using a frequency range without splitting oscillation humps (Gerster et al., 2022); and (3) the beta hump in our data profile ended at approximately 25 Hz (Figure 2a). Because two oscillation peaks (alpha and beta) were clearly visible at the low band (Figure 2a), we specified the number of maximum peaks as 2 when fitting the low-band $1/f$ parameters and 0 when fitting the high-band $1/f$ parameters in FOOOF (Donoghue et al., 2020).

The second treatment is that we introduce a parameter that specifically models the bending feature of the spectrum in the log–log space. To model this bending feature, the FOOOF method introduces a parameter

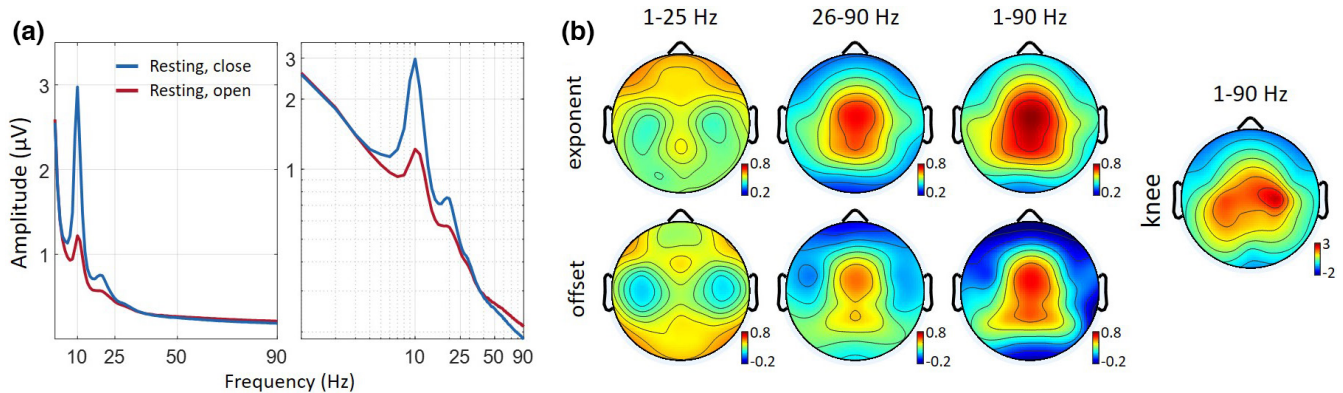


FIGURE 2 Grand average amplitude spectra and spatial distributions of the $1/f$ parameters. (a) Grand average amplitude spectra from the two resting states plotted in linear (left) and log–log (right) spaces (averaged across all participants, electrodes, and epochs). (b) Spatial distributions of the grand average $1/f$ parameters fit from different procedures.

k in the following equation describing the aperiodic component:

$$L = b - \log(k + F^\chi)$$

where b is the broadband offset, χ is the exponent and k is the “knee” parameter, controlling for the bend in the aperiodic component (Donoghue et al., 2020). The higher the k is, the more curved the spectrum is in the log–log space protruding towards the top-right direction. After fitting the entire aperiodic component with these three parameters, k (bending), χ (exponent/slope) and b (offset), they were separately fed to the statistical analysis concerning their relationships with the cognitive abilities. For naming simplicity, the $1/f$ parameters derived from the two bands will be termed as low-band (1–25 Hz) and high-band (26–90 Hz) $1/f$ parameters, and the $1/f$ parameters from the fitting of whole spectrum with a knee parameter will be termed as whole-band $1/f$ parameters.

The $1/f$ parameters were estimated based on the three average spectra at the single-electrode level for each participant. For each participant, three values of each $1/f$ parameter were obtained from the three equally separated data segments (further averaged across electrodes) to serve as the three indicators for constructing latent variables in structural equation modeling (see Structural Equation Modeling section for more details).

2.2.4 | Performance evaluation of cognitive tasks

The performance of each cognitive task was evaluated based on the mean RT across all correctly responded trials. To construct a latent variable for each cognitive ability in structural equation modeling (see the Structural Equation

Modeling section for more details), we categorized all trials in each task into two or three equal partitions and obtained the mean RTs of the correct trials within each partition. P-SRT, M-SRT, VSWM, and MC were separated into three equal partitions (i.e., 10 trials in each partition) according to the trial order. TS was separated into two partitions—30 repetition trials and 30 switching trials (see Task #3: Task-switching Task section for more details)—because the two trial types were heterogeneous in difficulty.

When calculating the mean RT of the correct trials within each partition, we performed the following procedures. For each partition, we first extracted the correctly responded trials and obtained their RTs; then, we eliminated the RTs that were more than $2 \times$ inter-quartile range above the 3rd quartile or below the 1st quartile (implemented through the built-in function of *isoutlier* in MATLAB); finally, we averaged the remaining RTs to obtain the mean RT as an indicator of response speed for each partition. Only the performance of the correct trials was evaluated because, compared with incorrect trials, correct trials are more able to represent genuine cognitive ability. Considering that the RTs from most cognitive tasks display ex-Gaussian distribution (Schmiedek et al., 2007) with right skewness, we additionally applied reciprocal transformation to the RTs and examined the robustness of the statistical results between these two versions of behavioral data (i.e., RT and $1/RT$).

2.2.5 | Structural equation modeling

SEM was applied to investigate the latent-level correlations between the scale-free dynamics characterized by the resting-state EEG task and the cognitive abilities assessed through the cognitive tasks.

The SEM models were constructed to examine the cognitive associations of scale-free dynamics. Basically,

in each of the SEM model, one scale-free parameter factor (built from three indicators) as well as gender and age serve as the independent variable in the regression, and factors of cognitive abilities (built from two or three indicators, see the diagram in Figure 3) serve as dependent variables. As the $1/f$ parameters were obtained from different ways of fitting (see above), the SEM results for all of them will be separately reported. Of note, all the factors included in our SEM models were constructed from equally

separated partitions of measurement data. The number of indicators for constructing the latent factors was decided heuristically (Little et al., 1999). Little et al. (1999, p. 206) noted that a small number of indicators (two or three) “may suffice to identify the construct of a latent factor precisely” when a measurement is well-specified and homogeneous. Given that the number of trial samples in the present data was limited, we used a minimal number of indicators when constructing our SEM models.

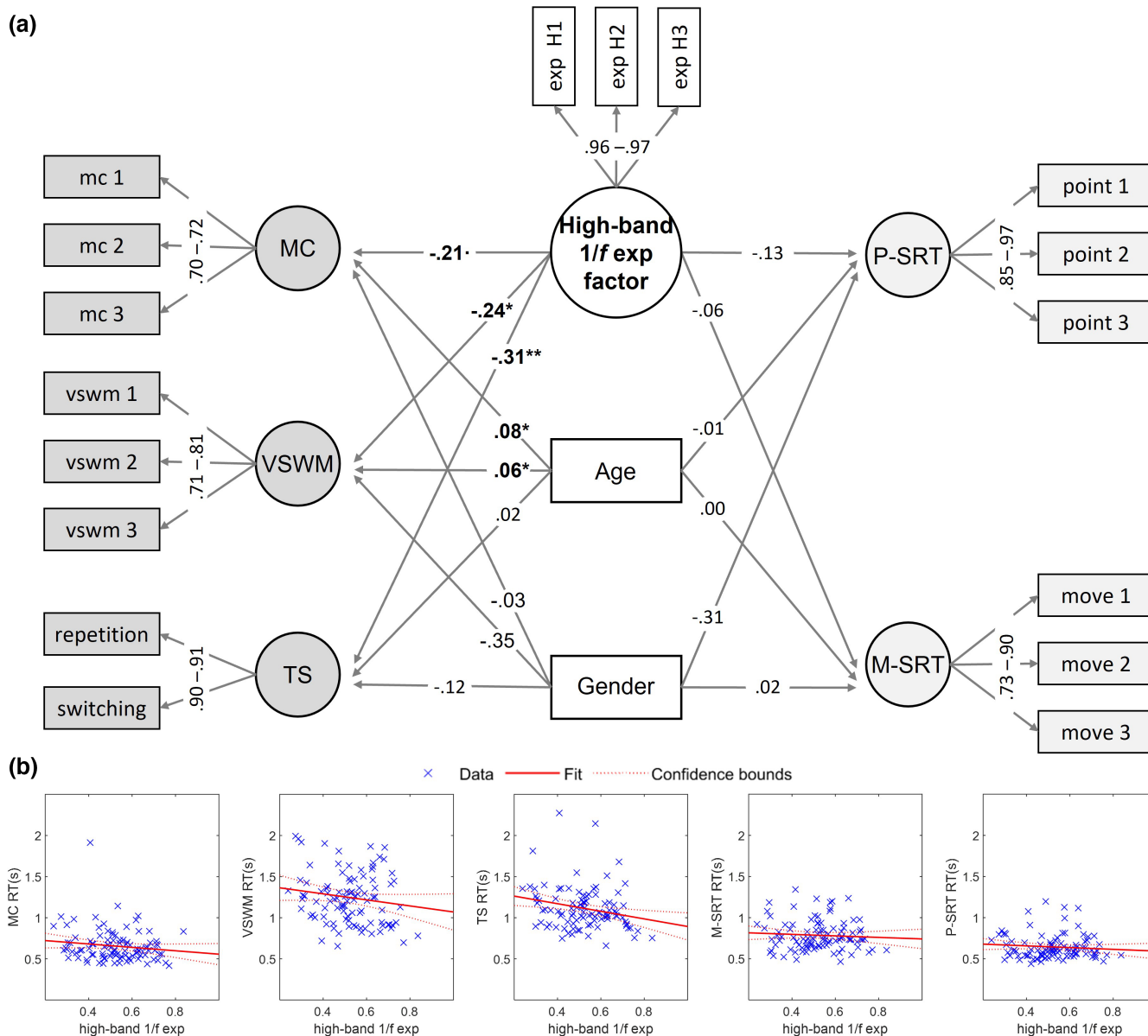


FIGURE 3 SEM results based on the factor of high-band $1/f$ exponent. (a) Schematic representation of the SEM model that correlates the high-band $1/f$ exponent factor and cognitive ability factors. The correlations between all of the factors and the range of factor loadings are shown in the figure. Model fit indices: CFI = 0.966, RMSEA = 0.063, and SRMR = 0.055. (b) Scatter plots of the high-band $1/f$ exponent against the behavioral performance of the five cognitive abilities. The data points were obtained by averaging all indicators within each latent factor. Correlation estimates with $p < .1$ are shown in boldface (** $p < .01$, * $p < .05$, $p < .1$). The two low-level cognitive ability factors are denoted with a light-gray background, and the three high-level cognitive ability factors are denoted with a dark-gray background. MC, mental calculation task; VSWM, visuospatial working memory task; TS, task-switching task; P-SRT, pointing-arrow simple reaction time task; M-SRT, moving-arrow simple reaction time task; RT, reaction time; exp, exponent; H, high band.

To indicate the goodness-of-fit of the SEM models, we used the following three widely accepted fit indices (Bentler, 1990; Hu & Bentler, 1999), comparative fit index (CFI), root mean square error of approximation (RMSEA) and standardized root mean square residual (SRMR). The SEM analysis was performed using the R package *lavaan* (R Development Core Team, 2010; Yves, 2012).

3 | RESULTS

3.1 | Descriptive statistics of behavioral performance in the cognitive tasks

Table 1 summarized the descriptive statistics of behavioral performance in the five cognitive tasks.

3.2 | Visualization of resting-state spectra and parameterization of 1/f component

The grand average amplitude spectra of the eyes-open and eyes-closed resting states are shown in Figure 2a. A significant enhancement in the power of the alpha band (at

approximately 10 Hz) was clearly seen in the eyes-closed state compared with that in the eyes-open state. This clear Berger effect confirmed the validity of the resting-state EEG recordings collected in this study.

The scalp maps of the grand average 1/f exponent parameters estimated from the low-band, high-band, and whole-band spectra are shown in Figure 2b. The high-band 1/f exponent showed a spatial distribution with a peak magnitude in the central scalp area petering towards the edges. In contrast, the low-band 1/f exponent displayed a special spatial distribution with a relatively larger magnitude in the prefrontal and parietal regions and a visibly lower magnitude in the temporal regions. As for the goodness of fit, the average R² for the three fitting procedures described in Method section (low-band, high-band, whole-band with knee parameters) was 0.93, 0.61, and 0.95, respectively.

3.3 | Estimating latent-level correlations between scale-free dynamics and cognitive abilities at different levels

To estimate the associations between scale-free dynamics and cognitive abilities at different levels, we constructed SEM models with six factors from multiple indicators and

Level of cognitive process	Cognitive task	Partition	Reaction time (s)		Accuracy	
			Mean	SD	Mean (%)	SD
Low-level automatic process	Pointing-arrow simple reaction time task (P-SRT)	Total	0.65	0.15	96.3	1.14
		Partition 1	0.71	0.19	94.0	0.71
		Partition 2	0.62	0.14	97.0	0.58
		Partition 3	0.60	0.13	97.9	0.55
Low-level automatic process	Moving-arrow simple reaction time task (M-SRT)	Total	0.79	0.18	95.5	1.16
		Partition 1	0.91	0.26	94.5	0.68
		Partition 2	0.75	0.20	96.3	0.66
		Partition 3	0.70	0.16	95.8	0.60
High-level controlled process	Task-switching task (TS)	Total	1.12	0.26	96.7	1.55
		Partition (switching)	1.11	0.28	96.4	1.12
		Partition (repetition)	1.13	0.26	97.0	0.99
High-level controlled process	Visuospatial working memory (VSWM)	Total	1.25	0.34	85.4	2.35
		Partition 1	1.31	0.39	85.0	1.22
		Partition 2	1.24	0.41	85.3	1.11
		Partition 3	1.19	0.36	85.9	1.07
High-level controlled process	Mental calculation (MC)	Total	0.66	0.20	92.9	1.51
		Partition 1	0.67	0.28	92.5	0.79
		Partition 2	0.66	0.23	93.6	0.81
		Partition 3	0.64	0.19	92.5	0.74

TABLE 1 Descriptive statistics of performance in each cognitive task.

two control variables. As shown in Figure 3, the five cognitive abilities were modeled as separate factors, and each was set to be predicted by a scale-free factor (i.e., $1/f$ factor constructed from specific $1/f$ parameters) and two control variables (i.e., gender and age).

Figure 3 exemplifies the SEM model for the high-band $1/f$ exponent parameters (26–90 Hz). This model shows that the variability of the high-band scale-free factor only significantly predicted individual differences in certain cognitive abilities. Particularly, the pattern shows that the high-level abilities (MC, VSWM, TS) are strongly predicted by the scale-free factor, whereas the low-level abilities (P-SRT, M-SRT) are not. For all the three significant predictions, the relationships all show that higher exponent (steeper slope) is associated with shorter RT (thus better performance). This relationship is better visualized in the scatter plots of the variable pairs (Figure 3b).

The embedded numerals in Figure 3 are only for the factor of high-band $1/f$ exponent. We now show how the relationships between different scale-free parameters and

different levels of cognitive abilities vary across different ways of fitting and summarize the consistency and patterns therein. As described in Method section, we implemented three ways of fitting the aperiodic component with FOOOF: (1) fitting a straight line within the low band of 1–25 Hz, (2) fitting a straight line within the high band of 26–90 Hz, (3) fitting a “bent” line to the whole band of 1–90 Hz. For the first two fittings, two $1/f$ parameters (exponent and offset) were obtained. For the third fitting, three $1/f$ parameters (exponent, offset, and knee) were obtained. It is important to note that the knee parameter k is a value that controls the degree of bending, not a knee point that breaks the straight line into two segments separated at k Hz (Donoghue et al., 2020). Table 2 summarizes the SEM fitting results for all the $1/f$ parameters from the three different fitting ways.

The most conspicuous pattern from Table 2 is that the $1/f$ parameters overwhelmingly predict the high-level ability factors (MC, VSWM, TS), but not the low-level ones (P-SRT, M-SRT). There are indeed some sporadic substantial

TABLE 2 SEM results for different $1/f$ factors.

	High-level			Low-level		CFI	RMSEA	SRMR
	MC	VSWM	TS	P-SRT	M-SRT			
Based on RT								
Low-band								
Exponent	0.03 (0.78)	0.09 (0.42)	0.12 (0.26)	0.15 (0.16)	0.07 (0.53)	0.97	0.06	0.05
Offset	-0.27 (0.033)	-0.17 (0.15)	-0.06 (0.56)	-0.01 (0.96)	0.04 (0.70)	0.96	0.06	0.07
High-band								
Exponent	-0.21 (0.076)	-0.24 (0.041)	-0.31 (0.005)	-0.13 (0.22)	-0.06 (0.58)	0.97	0.06	0.06
Offset	-0.29 (0.020)	-0.26 (0.032)	-0.32 (0.005)	-0.18 (0.096)	-0.08 (0.49)	0.96	0.07	0.07
Whole-band + knee								
Exponent	-0.27 (0.026)	-0.35 (0.004)	-0.33 (0.003)	-0.13 (0.22)	-0.02 (0.86)	0.98	0.05	0.05
Offset	-0.22 (0.06)	-0.34 (0.006)	-0.28 (0.012)	-0.11 (0.30)	0.01 (0.92)	0.98	0.05	0.06
Knee	-0.23 (0.06)	-0.30 (0.015)	-0.33 (0.004)	-0.28 (0.011)	-0.11 (0.32)	0.97	0.05	0.05
Based on 1/RT								
Low-band								
Exponent	-0.06 (0.58)	-0.16 (0.15)	-0.17 (0.098)	-0.19 (0.067)	-0.04 (0.68)	0.97	0.06	0.04
Offset	0.18 (0.12)	0.14 (0.22)	0.09 (0.43)	-0.01 (0.93)	-0.01 (0.94)	0.97	0.06	0.06
High-band								
Exponent	0.22 (0.045)	0.22 (0.046)	0.34 (0.002)	0.15 (0.16)	0.05 (0.59)	0.98	0.06	0.05
Offset	0.27 (0.020)	0.26 (0.029)	0.37 (0.001)	0.21 (0.054)	0.09 (0.42)	0.97	0.06	0.06
Whole-band + knee								
Exponent	0.28 (0.014)	0.34 (0.003)	0.39 (0.001)	0.15 (0.15)	-0.01 (0.97)	0.97	0.06	0.05
Offset	0.23 (0.040)	0.32 (0.006)	0.34 (0.003)	0.14 (0.18)	-0.04 (0.70)	0.97	0.06	0.05
Knee	0.30 (0.010)	0.34 (0.004)	0.41 (0.001)	0.32 (0.005)	0.13 (0.24)	0.97	0.06	0.05

Note: The upper half is based on RT. The lower half is based on 1/RT. The first five columns are the β values of the regression describing the degree the $1/f$ parameters predict the cognitive ability factors (age and gender were involved all along as shown in Figure 3). The associated p values are provided in the parentheses after the β values. The values with $p < .1$ are shown in boldface.

β s in low-level ability factors, which is only in P-SRT (only robustly shown in its association with the knee parameter). In terms of the variation across the frequency bands, the effects of $1/f$ parameters are predominantly located in the high-band and are weakly captured by the low-band spectrum. In terms of the direction of the effect, it is always that lower RT (higher ability) is associated with a larger exponent (steeper slope of the $1/f$ pattern), higher offset, and higher knee (bending more towards the top-right direction). Note the opposite signs of the effect values between the top and bottom panels. This is due to the transformation of RT to $1/RT$. The effect of transforming RT to $1/RT$ is shown in Figure 4. Finally, the results did

not substantially differ after we introduced the task order of P-SRT, M-SRT, and TS as a control variable.

4 | DISCUSSION

4.1 | Summary

The present study delineated the cognitive associations of resting-state scale-free neural dynamics in the complex human cognitive system by testing whether resting-state scale-free dynamics predict individual differences in the various cognitive abilities that involve two distinct levels

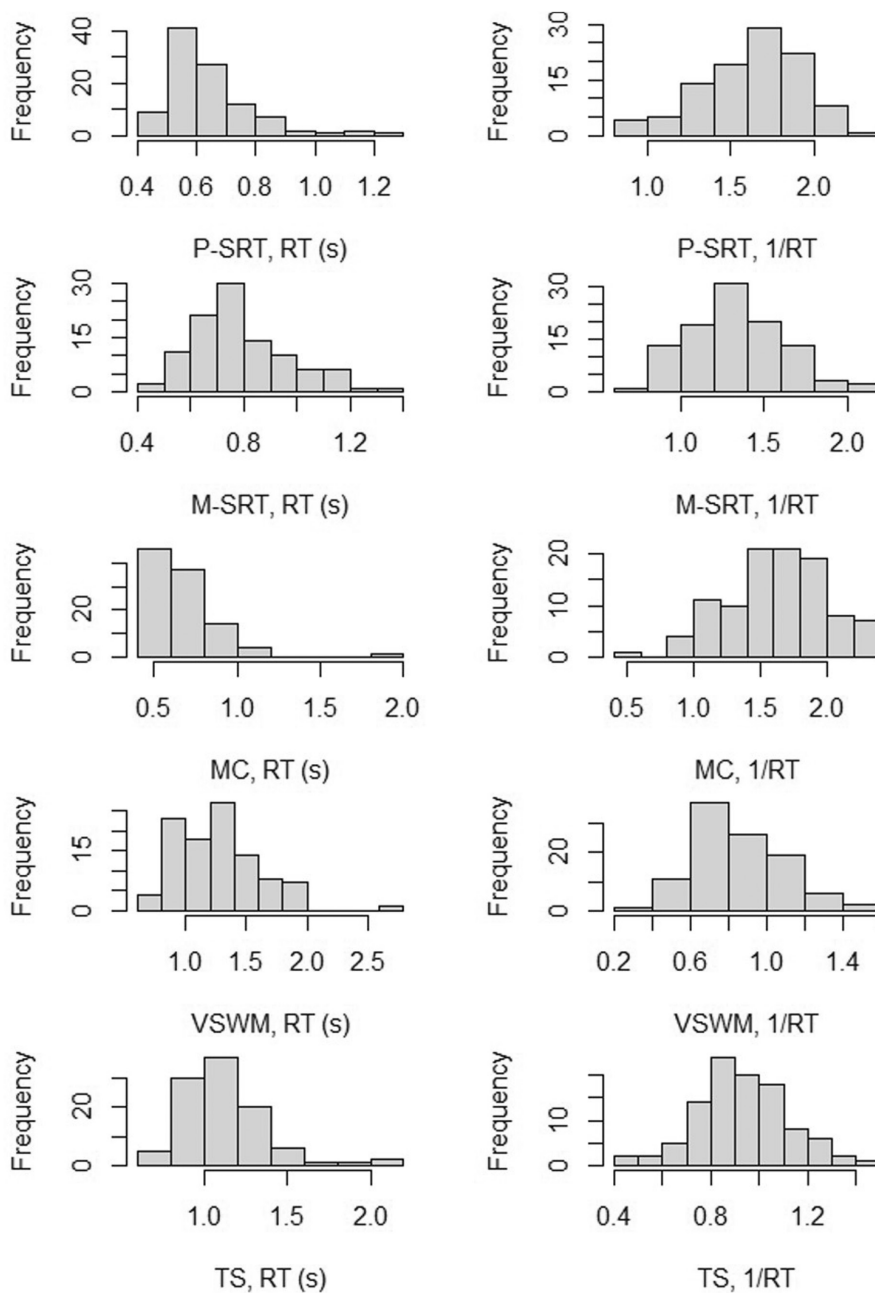


FIGURE 4 Distribution of reaction time (RT) and its transformation (1/RT) across participants for different tasks.

of cognitive process (i.e., low-level automatic processes and high-level controlled processes). Based on a series of tasks specifically designed to address this question and quantitative analyses based on SEM, we found that (1) resting-state scale-free dynamics significantly predicted individual differences in cognitive abilities involving high-level controlled processes, but appeared to be only weakly associated with low-level automatic processes (primarily the sensorimotor process) and (2) the cognitive association of scale-free dynamics was mainly attributable to the high band (26–90 Hz) but not the low band (1–25 Hz) 1/*f* spectral component.

4.2 | Task design for measuring cognitive processes at different levels

To investigate how the associations between resting-state scale-free dynamics and cognitive abilities differ across different levels of the cognitive system, first, we designed tasks that evoked different levels of cognitive processes but were homogeneous in other aspects. Based on dual-process theory, we adopted a framework that proposes two distinct types of human cognitive processes: automatic and controlled. Dual-process theory has been well established and supported by a large body of theoretical and empirical studies (for a review, see Evans & Stanovich, 2013) as well as computational simulations (Milli et al., 2021). Given that the defining distinction between the two types of processes lies in the demand for working memory resources, the common experimental design to create tasks testing the two different processes is to manipulate the task demand of working memory (Evans & Stanovich, 2013). Our task design measuring high- and low-level cognitive processes made use of this principle of dual-process theory.

However, it is challenging to eliminate all confounding factors between the two levels of cognitive tasks if a substantial amount of task content (e.g., stimulus) is already different. We adopted the TS paradigm to address this issue; although the TS design serves as a mechanism to induce controlled processes by requiring participants to switch back and forth between two task conditions, each one of the two conditions can serve as an ideal single task for measuring low-level sensorimotor-dominating task that mainly involves automatic processes. The pivotal element of our design here was that the two separate tasks (P-SRT and M-SRT) shared entirely identical stimulus contents as TS, effectively eliminating the confounding factors in task content. Furthermore, our TS design blended the cues (for instructing which task condition to perform) into the stimulus itself, different from the TS designs that involve separate cues (Kiesel et al., 2010). Presumably, this blending would increase cognitive demand owing

to the simultaneous processing of the cues and stimulus contents. Another advantage of our blending design was that it guaranteed the identity of the stimulus contents between high-level (TS) and low-level (P-SRT and M-SRT) tasks because no cue was needed in the latter.

Taken together, the novel design of P-SRT, M-SRT, and TS enabled us to differentiate cognitive processes at different levels without any chance of confounding with other factors (e.g., stimulus content). Finally, the inclusion of the other two high-level tasks (although not controlled for stimulus content), MC and VSWM, and their significant association with the scale-free parameters further supported the differentiation between high and low-level cognitive systems in terms of their implication with scale-free dynamic features. It is noted that the RTs for MC are substantially shorter than the other two high-level tasks (TS and VSWM). This is mainly due to the task design: before the presentation of the last frame, the participants (especially those proficient ones) would have already finished the calculation and obtained the answer. Therefore, what they did was simply comparing the answer in mind and the number shown. Nevertheless, this task would still be able to reflect high-level cognitive performance because those participants less efficient in MC have a higher chance to stay in the calculation when the last frame shows. Overall, the task design led to a “leakage” of mental process to the previous stages, which resulted in shorted RTs but retained the cross-individual variability in MC ability.

4.3 | Relationship between scale-free neural dynamics and cognitive abilities at different levels

The search for robust neural biomarkers for cognitive function in cognitive neuroscience is ongoing. Although many neural metrics, including both anatomical and functional aspects, have been reported to be indicative of various cognitive abilities (Anderson & Perone, 2018; Cheron et al., 2016; Cole et al., 2016; Goswami, 2009; Harris et al., 2020; Penke et al., 2012; Supekar et al., 2013), the findings in the field are heterogeneous. In recent years, scale-free neural dynamics have developed as a noticeable area in this line of research because numerous studies have identified their ability to predict various cognitive abilities (see the review in the Introduction section). However, given the complexity of the brain and the cognitive system, it is difficult to conceive of the existence of a universal neural indicator of general cognitive ability. Therefore, we hypothesized that a fine-grained structure should exist in the cognitive association of scale-free dynamics; that is, the association may be influenced by the level of cognitive processing of subjects.

Given the previously claimed implication of scale-free dynamic features with the complexity of nonlinear dynamic systems, particularly those self-sustained dynamic systems showing the ability to flexibly cope with uncertain inputs and non-prescribed routines (Cavanna et al., 2018; Cocchi et al., 2017; Kelso, 2012), we hypothesized that scale-free dynamics should be more likely to predict cognitive abilities involving high-level controlled processes. Accordingly, we designed tasks that could examine the differential associations between scale-free dynamics and cognitive abilities at different levels (see the previous section). In line with our hypothesis, we found that resting-state scale-free dynamics exclusively predicted the cognitive abilities mainly involving high-level controlled processes but were only weakly associated with low-level automatic processes. Our results corroborate those of numerous studies reporting the significant prediction effects of scale-free dynamics on tasks that demand strenuous executive control (Bongers et al., 2020; Huang et al., 2016; Immink et al., 2021; Kasagi et al., 2017; Kolvoort et al., 2020; Ouyang et al., 2020). As for the low-level cognitive abilities, to the best of our understanding, the results of our study showed, for the first time, that scale-free neural dynamics are weakly associated with cognitive abilities primarily involving the low-level sensorimotor automatic processes. This dichotomous phenomenon observed in our study may connect complex system theory to dual-process theory: According to dual-process theory, the automatic process is rooted in a primitive functional system that is hard-wired, deterministic, and highly habitual, leaving little room for variability. Therefore, low variability or complexity (in the sense of self-organized, nonlinear, and adaptive biological systems) is needed. In contrast, controlled processes feature cognitive flexibility to cope with changing contexts (Evans & Stanovich, 2013), which is one of the defining features of complex dynamic systems (Cavanna et al., 2018; Cocchi et al., 2017; Kelso, 2012). Based on the theory that scale-free dynamics reflect a system's complexity and flexibility (Cocchi et al., 2017), scale-free dynamics are justifiably only associated with high-level but not low-level cognitive abilities.

4.4 | Possible interpretation of the relationships at a mechanistic level

Despite the well-acknowledged functional significance, its generative mechanism of scale-free dynamics in the brain remains largely unclear (Lendner et al., 2020). Various hypotheses have been proposed, including self-organized criticality, balance of excitation and inhibition (E/I) in neural circuits, low-pass dendritic filtering, and asynchronous neuronal firing (Bak et al., 1987; Cocchi et al., 2017; Gao et al., 2017; Lindén et al., 2010; Miller

et al., 2009). Among these, self-organized criticality appears to have received the most attention and discussion (Cocchi et al., 2017). In brief, self-organized criticality indicates that scale-free brain activity manifests a dynamic criticality state between order and disorder, which is a critical point at which various functions, including “information transmission, information storage, dynamic range, metastable states, and computational power,” achieve an optimal state (Zimmern, 2020). However, this theory only states that the optimal functional states are associated with the scale-freeness of the dynamic activity, thus is still limited in explaining the data relationships in the current study about the characteristic parameters of scale-free pattern. Here, scale-freeness refers to the feature of the power spectrum being scale-free (being straight in the log–log space), and characteristic parameters of scale-free pattern refer to those describing the characteristics of the pattern, particularly, the exponent. One possibility for the present results to be linked to scale-freeness (thus criticality) is that the characteristic parameters are implicated with the scale-freeness of temporal dynamics: non-criticality dynamics (e.g., super-criticality and sub-criticality) shape the $1/f$ exponent estimation by making it deviate from $1/f$ pattern (Liang & Zhou, 2022), and such a distortion ought to bias the characteristic parameters. This effect leaves an open question regarding how the characteristic parameters are influenced by sub-criticality or super-criticality features in the EEG data.

Another possible mechanistic interpretation is the excitation/inhibition (E-I) balance theory, which is particularly linked to the exponent parameter. Gao et al., 2017 presented a neural model with tunable E-I balance which showed that the strength of inhibitory synapses in the simulated neural network determines the slope of the $1/f$ spectrum—the higher inhibition the steeper slope. The mechanism was later reported to be consistent with the phenomenon that decreased arousal states are associated with increased inhibition. If the neuronal inhibition account holds true, it implies that higher ability in controlled tasks is associated with stronger inhibition, which is conceptually compatible with the cognitive theory that inhibitory control is one of the core executive functions (Miyake et al., 2000).

Finally, although the current article as well as the majority of previous work on $1/f$ -cognition relationships drew particular attention on the exponent of the $1/f$ pattern (Bongers et al., 2020; Cross et al., 2022; Huang et al., 2016; Kardan et al., 2020; Kasagi et al., 2017; Ouyang et al., 2020; Waschke et al., 2021), it is important to note that the offset has also been found to be significantly associated with various cognitive abilities (Clements et al., 2021; Immink et al., 2021; Waschke et al., 2021; Zhang et al., 2021). In the present work, the offset displays a similar feature to the exponent in terms of its differential relationships with

high- and low-level abilities. In some cases, the association in the offset is even stronger than the exponent. This points to the fact that the offset parameter—although not the core defining feature of $1/f$ or scale-free dynamics—plays an important role and should not be neglected. Actually, the involvement of offset in the association with cognitive abilities implies that scale-freeness is likely not the sole account for the cognitive variability.

4.5 | Scale-free neural dynamics in different frequency bands

Although extensive research has demonstrated the functional relevance of scale-free neural dynamics, the spectra of neural activity at different levels do not strictly exhibit a power law pattern (Chaudhuri et al., 2017; Donoghue et al., 2020; He, 2014; He et al., 2010; Lendner et al., 2020). The scale-free feature has been commonly reported to reflect a certain frequency band depending on the type, level, or modality of neural data (He, 2011). Surprisingly, there is no established standard or rule of thumb specifying which frequency range should be used to estimate the $1/f$ slope in different contexts. Various reasons have been reported for frequency selection. For example, some studies have used a range of approximately 1–40 Hz to exclude contamination from ocular and motor artifacts (Colombo et al., 2019; Immink et al., 2021; Kardan et al., 2020; Ouyang et al., 2020); other studies have recommended a frequency range in which no pronounced oscillatory activity and “knee” points are presented, for example, a low-frequency range of below 20 Hz or a high-frequency range greater than 30 Hz to avoid the clear “knee” at approximately 20 Hz (Colombo et al., 2019; Gao et al., 2017; Lendner et al., 2020); moreover, some studies have used very low bands without providing explicit reasons (Lei et al., 2015).

If the spectrum displays a non-straight pattern in the log–log axes, it is reasonable to assume differential functional signatures in different local bands that show in-band straight patterns. Scale-free neural dynamics in different frequency ranges have been shown to be based on different generative mechanisms (He et al., 2010; Lendner et al., 2020; Miller et al., 2009). In addition to the differential associations with cognitive abilities, the different spatial distributions of the $1/f$ slope from the different bands served as another strong piece of evidence. The distributions of the high-band $1/f$ slopes exhibited a more centralized and broader coverage of the frontal–central–parietal area (Figure 2b). In contrast, the low-band $1/f$ slopes showed a radically different pattern, suggesting a different underlying network. These differences led us to compare the prediction effects obtained from the low-band and high-band $1/f$ slopes split at 25 Hz. As expected, the frequency

range crucially determined the prediction effects of scale-free dynamics on cognitive abilities. In the present case, only the high-band $1/f$ slope was predictive of cognitive abilities. This corroborates the findings of previous studies that the $1/f$ slope fitted from >30 Hz is substantially more indicative of variation in the mental state than that fitted from <20 Hz (Gao et al., 2017; Lendner et al., 2020).

However, it has to be noted that our treatment of separating the $1/f$ fitting into the two bands separated at 25 Hz only serves to reveal the different cognitive associations between low and high bands, not to suggest that the exact value of 25 Hz bears theoretical or functional signatures. This also highlights another fundamental issue in the use of the term “scale-free” throughout the article. The terminology of “scale-free” actually goes against the idea of estimating relevant parameters in a band-confined (thus, scale-not-free) manner, which is an issue existing in all similar studies in the literature. One argument for this issue is that researchers can use reality-restricted data features to estimate a theoretical construct. It appears that a specific frequency band needs to be specified for estimating the theoretical construct of scale-freeness owing to the fact that the low end and high end are shaped by biological or technical constraints (Gerster et al., 2022). Another way to explicitly model the non-straightness is to introduce an additional parameter characterizing this feature into the fitting. The FOOOF method allows to add this bending parameter k and after fitting the k -included aperiodic model to every individual, we further confirmed that that scale-free parameters were predominantly associated with the high-level cognitive abilities.

An additional note about the results of data fit in different frequency bands is that the goodness of fit showed to be much lower in the high-frequency band ($R^2 = .61$) as compared to the fits in the low band and whole band (both $R^2 > .9$). We would like to note that this could be partly due to the intrinsic pattern of the spectrum. As shown in (Donoghue et al., 2020, particularly in Figure 2), the goodness fit R^2 in FOOOF was calculated on the original power spectrum density (PSD) based on a natural (rather than logarithmic) scale of frequency axis. Under this scale, PSD curve is flatter in higher frequency band, which will lead to lower explanation of the variance (vertical dispersion) by the fit curve.

5 | CONCLUSION

This study advanced our understanding of the cognitive associations of resting-state scale-free neural dynamics by demonstrating that resting-state scale-free dynamics are not a universal neural indicator of all cognitive abilities but exhibit a structured relationship related to the level of cognitive

processes. Moreover, we reported that scale-free neural dynamics at different frequency ranges showed different associations with cognitive ability. Future studies investigating the associations between scale-free dynamics and cognitive abilities should pay special attention to the level of cognitive ability as well as the frequency range used for parameterizing the scale-free properties. In future studies, a more detailed structure of the relationships between scale-free neural dynamics and the complete cognitive system should be revealed using a more fine-grained factorized task design, which will benefit the understanding of the mechanisms via which scale-free neural dynamics support cognition.

AUTHOR CONTRIBUTIONS

Leisi Pei: Data curation; formal analysis; investigation; methodology; visualization; writing – original draft; writing – review and editing. **Xinlin Zhou:** Writing – review and editing. **Frederick Koon Shing Leung:** Writing – review and editing. **Guang Ouyang:** Funding acquisition; methodology; project administration; supervision; writing – review and editing.

FUNDING INFORMATION

This work was partially supported by the Hong Kong Research Grant Council (27603818 and 17609321).

CONFLICT OF INTEREST

The authors declare no competing interests.


DATA AVAILABILITY STATEMENT

The data and codes that support the findings of this study are available from the corresponding author upon request.

ORCID

Leisi Pei  <https://orcid.org/0000-0002-1641-1600>

Xinlin Zhou  <https://orcid.org/0000-0002-3530-0922>

Frederick K. S. Leung  <https://orcid.org/0000-0003-1725-3883>

Guang Ouyang  <https://orcid.org/0000-0001-8939-7443>

REFERENCES

- Allegrini, P., Menicucci, D., Bedini, R., Fronzoni, L., Gemignani, A., Grigolini, P., West, B. J., & Paradisi, P. (2009). Spontaneous brain activity as a source of ideal $1/f$ noise. *Physical Review E*, 80(6), 061914. <https://doi.org/10.1103/PhysRevE.80.061914>
- Anderson, A. J., & Perone, S. (2018). Developmental change in the resting state electroencephalogram: Insights into cognition and the brain. *Brain and Cognition*, 126, 40–52. <https://doi.org/10.1016/j.bandc.2018.08.001>
- Bak, P., Tang, C., & Wiesenfeld, K. (1987). Self-organized criticality: An explanation of the $1/f$ noise. *Physical Review Letters*, 59(4), 381–384. <https://doi.org/10.1103/PhysRevLett.59.381>
- Barry, R. J., Clarke, A. R., Johnstone, S. J., Magee, C. A., & Rushby, J. A. (2007). EEG differences between eyes-closed and eyes-open resting conditions. *Clinical Neurophysiology*, 118(12), 2765–2773. <https://doi.org/10.1016/j.clinph.2007.07.028>
- Bazanov, O. M., & Vernon, D. (2014). Interpreting EEG alpha activity. *Neuroscience & Biobehavioral Reviews*, 44, 94–110. <https://doi.org/10.1016/j.neubiorev.2013.05.007>
- Beggs, J., & Timme, N. (2012). Being critical of criticality in the brain. *Frontiers in Physiology*, 3, 163. <https://doi.org/10.3389/fphys.2012.00163>
- Beggs, J. M. (2008). The criticality hypothesis: How local cortical networks might optimize information processing. *Philosophical Transactions of the Royal Society A: Mathematical, Physical and Engineering Sciences*, 366(1864), 329–343. <https://doi.org/10.1098/rsta.2007.2092>
- Bentler, P. M. (1990). Comparative fit indexes in structural models. *Psychological Bulletin*, 107(2), 238–246. <https://doi.org/10.1037/0033-2909.107.2.238>
- Bongers, A., Flynn, A. B., & Northoff, G. (2020). Is learning scale-free? Chemistry learning increases EEG fractal power and changes the power law exponent. *Neuroscience Research*, 156, 165–177. <https://doi.org/10.1016/j.neures.2019.10.011>
- Cavanna, F., Vilas, M. G., Palmucci, M., & Tagliazucchi, E. (2018). Dynamic functional connectivity and brain metastability during altered states of consciousness. *NeuroImage*, 180, 383–395. <https://doi.org/10.1016/j.neuroimage.2017.09.065>
- Chaudhuri, R., He, B. J., & Wang, X.-J. (2017). Random recurrent networks near criticality capture the broadband power distribution of human ECoG dynamics. *Cerebral Cortex*, 28(10), 3610–3622. <https://doi.org/10.1093/cercor/bhx233>
- Cheron, G., Petit, G., Cheron, J., Leroy, A., Cebolla, A., Cevallos, C., Petieau, M., Hoellinger, T., Zarka, D., Clarinval, A. M., & Dan, B. (2016). Brain oscillations in sport: Toward EEG biomarkers of performance. *Frontiers in Psychology*, 7, 246. <https://doi.org/10.3389/fpsyg.2016.00246>
- Churchill, N. W., Spring, R., Grady, C., Cimprich, B., Askren, M. K., Reuter-Lorenz, P. A., Jung, M. S., Peltier, S., Strother, S. C., & Berman, M. G. (2016). The suppression of scale-free fMRI brain dynamics across three different sources of effort: Aging, task novelty and task difficulty. *Scientific Reports*, 6(1), 30895. <https://doi.org/10.1038/srep30895>
- Clements, G. M., Bowie, D. C., Gyurkovics, M., Low, K. A., Fabiani, M., & Gratton, G. (2021). Spontaneous alpha and theta oscillations are related to complementary aspects of cognitive control in younger and older adults. *Frontiers in Human Neuroscience*, 15(106), 621620. <https://doi.org/10.3389/fnhum.2021.621620>
- Cocchi, L., Gollo, L. L., Zalesky, A., & Breakspear, M. (2017). Criticality in the brain: A synthesis of neurobiology, models and cognition. *Progress in Neurobiology*, 158, 132–152. <https://doi.org/10.1016/j.pneurobio.2017.07.002>
- Cole, M. W., Ito, T., Bassett, D. S., & Schultz, D. H. (2016). Activity flow over resting-state networks shapes cognitive task activations. *Nature Neuroscience*, 19(12), 1718–1726. <https://doi.org/10.1038/nn.4406>
- Colombo, M. A., Napolitani, M., Boly, M., Gosseries, O., Casarotto, S., Rosanova, M., Brichant, J. F., Boveroux, P., Rex, S., Laureys, S., Massimini, M., Chiergato, A., & Sarasso, S. (2019). The spectral exponent of the resting EEG indexes the presence of consciousness during unresponsiveness induced by propofol, xenon, and ketamine. *NeuroImage*, 189, 631–644. <https://doi.org/10.1016/j.neuroimage.2019.01.024>

- Craik, F. I. M., & Lockhart, R. S. (1972). Levels of processing: A framework for memory research. *Journal of Verbal Learning and Verbal Behavior*, *11*(6), 671–684. [https://doi.org/10.1016/S0022-5371\(72\)80001-X](https://doi.org/10.1016/S0022-5371(72)80001-X)
- Cross, Z. R., Corcoran, A. W., Schlesewsky, M., Kohler, M. J., & Bornkessel-Schlesewsky, I. (2022). Oscillatory and aperiodic neural activity jointly predict language learning. *Journal of Cognitive Neuroscience*, *34*, 1630–1649. https://doi.org/10.1162/jocn_a_01878
- Dave, S., Brothers, T. A., & Swaab, T. Y. (2018). $1/f$ neural noise and electrophysiological indices of contextual prediction in aging. *Brain Research*, *1691*, 34–43. <https://doi.org/10.1016/j.brainres.2018.04.007>
- Delorme, A., & Makeig, S. (2004). EEGLAB: An open source toolbox for analysis of single-trial EEG dynamics including independent component analysis. *Journal of Neuroscience Methods*, *134*(1), 9–21. <https://doi.org/10.1016/j.jneumeth.2003.10.009>
- Donoghue, T., Haller, M., Peterson, E. J., Varma, P., Sebastian, P., Gao, R., Noto, T., Lara, A. H., Wallis, J. D., Knight, R. T., Shestyuk, A., & Voytek, B. (2020). Parameterizing neural power spectra into periodic and aperiodic components. *Nature Neuroscience*, *23*(12), 1655–1665. <https://doi.org/10.1038/s41593-020-00744-x>
- Duncan, J. (2010). The multiple-demand (MD) system of the primate brain: Mental programs for intelligent behaviour. *Trends in Cognitive Sciences*, *14*(4), 172–179. <https://doi.org/10.1016/j.tics.2010.01.004>
- Evans, J. S. B. T. (2011). Dual-process theories of reasoning: Contemporary issues and developmental applications. *Developmental Review*, *31*(2), 86–102. <https://doi.org/10.1016/j.dr.2011.07.007>
- Evans, J. S. B. T., & Stanovich, K. E. (2013). Dual-process theories of higher cognition: Advancing the debate. *Perspectives on Psychological Science: A Journal of the Association for Psychological Science*, *8*(3), 223–241. <https://doi.org/10.1177/1745691612460685>
- Fedorenko, E. (2014). The role of domain-general cognitive control in language comprehension. *Frontiers in Psychology*, *5*, 335. <https://doi.org/10.3389/fpsyg.2014.00335>
- Gao, R., Peterson, E. J., & Voytek, B. (2017). Inferring synaptic excitation/inhibition balance from field potentials. *NeuroImage*, *158*, 70–78. <https://doi.org/10.1016/j.neuroimage.2017.06.078>
- Gerster, M., Waterstraat, G., Litvak, V., Lehnertz, K., Schnitzler, A., Florin, E., Curio, G., & Nikulin, V. (2022). Separating neural oscillations from aperiodic $1/f$ activity: Challenges and recommendations. *Neuroinformatics*, *20*, 991–1012. <https://doi.org/10.1007/s12021-022-09581-8>
- Gifani, P., Rabiee, H. R., Hashemi, M. H., Taslimi, P., & Ghanbari, M. (2007). Optimal fractal-scaling analysis of human EEG dynamic for depth of anesthesia quantification. *Journal of the Franklin Institute*, *344*(3), 212–229. <https://doi.org/10.1016/j.jfranklin.2006.08.004>
- Gilmore, C., & Cragg, L. (2018). Chapter 14 – The role of executive function skills in the development of children’s mathematical competencies. In A. Henik & W. Fias (Eds.), *Heterogeneity of function in numerical cognition* (pp. 263–286). Academic Press.
- Goswami, U. (2009). Mind, brain, and literacy: Biomarkers as usable knowledge for education. *Mind, Brain, and Education*, *3*(3), 176–184. <https://doi.org/10.1111/j.1751-228X.2009.01068.x>
- Grigolini, P., Aquino, G., Bologna, M., Luković, M., & West, B. J. (2009). A theory of $1/f$ noise in human cognition. *Physica A: Statistical Mechanics and its Applications*, *388*(19), 4192–4204. <https://doi.org/10.1016/j.physa.2009.06.024>
- Gruber, O., Indefrey, P., Steinmetz, H., & Kleinschmidt, A. (2001). Dissociating neural correlates of cognitive components in mental calculation. *Cerebral Cortex*, *11*(4), 350–359. <https://doi.org/10.1093/cercor/11.4.350>
- Harris, S. E., Cox, S. R., Bell, S., Marioni, R. E., Prins, B. P., Pattie, A., Corley, J., Muñoz Maniega, S., Valdés Hernández, M., Morris, Z., John, S., Bronson, P. G., Tucker-Drob, E. M., Starr, J. M., Bastin, M. E., Wardlaw, J. M., Butterworth, A. S., & Deary, I. J. (2020). Neurology-related protein biomarkers are associated with cognitive ability and brain volume in older age. *Nature Communications*, *11*(1), 800. <https://doi.org/10.1038/s41467-019-14161-7>
- He, B. J. (2011). Scale-free properties of the functional magnetic resonance imaging signal during rest and task. *The Journal of Neuroscience*, *31*(39), 13786–13795. <https://doi.org/10.1523/JNEUROSCI.2111-11.2011>
- He, B. J. (2014). Scale-free brain activity: Past, present, and future. *Trends in Cognitive Sciences*, *18*(9), 480–487. <https://doi.org/10.1016/j.tics.2014.04.003>
- He, B. J., Zempel, J. M., Snyder, A. Z., & Raichle, M. E. (2010). The temporal structures and functional significance of scale-free brain activity. *Neuron*, *66*(3), 353–369. <https://doi.org/10.1016/j.neuron.2010.04.020>
- Hu, L. T., & Bentler, P. M. (1999). Cutoff criteria for fit indexes in covariance structure analysis: Conventional criteria versus new alternatives. *Structural Equation Modeling: A Multidisciplinary Journal*, *6*(1), 1–55. <https://doi.org/10.1080/10705519909540118>
- Huang, Z., Obara, N., Davis, H., Pokorny, J., & Northoff, G. (2016). The temporal structure of resting-state brain activity in the medial prefrontal cortex predicts self-consciousness. *Neuropsychologia*, *82*, 161–170. <https://doi.org/10.1016/j.neuropsychologia.2016.01.025>
- Immink, M. A., Cross, Z. R., Chatburn, A., Baumeister, J., Schlesewsky, M., & Bornkessel-Schlesewsky, I. (2021). Resting-state aperiodic neural dynamics predict individual differences in visuomotor performance and learning. *Human Movement Science*, *78*, 102829. <https://doi.org/10.1016/j.humov.2021.102829>
- James, W. (1890). *The principles of psychology* (Vol. 1). Henry Holt and Company.
- Kardan, O., Adam, K. C. S., Mance, I., Churchill, N. W., Vogel, E. K., & Berman, M. G. (2020). Distinguishing cognitive effort and working memory load using scale-invariance and alpha suppression in EEG. *NeuroImage*, *211*, 116622. <https://doi.org/10.1016/j.neuroimage.2020.116622>
- Kasagi, M., Huang, Z., Narita, K., Shitara, H., Motegi, T., Suzuki, Y., Fujihara, K., Tanabe, S., Kosaka, H., Ujita, K., Fukuda, M., & Northoff, G. (2017). Association between scale-free brain dynamics and behavioral performance: Functional MRI study in resting state and face processing task. *Behavioural Neurology*, *2017*, 2824615. <https://doi.org/10.1155/2017/2824615>
- Kelso, J. A. S. (2012). Multistability and metastability: Understanding dynamic coordination in the brain. *Philosophical Transactions of the Royal Society of London. Series B, Biological Sciences*, *367*(1591), 906–918. <https://doi.org/10.1098/rstb.2011.0351>
- Kiesel, A., Steinhauser, M., Wendt, M., Falkenstein, M., Jost, K., Philipp, A. M., & Koch, I. (2010). Control and interference in

- task switching—A review. *Psychological Bulletin*, 136(5), 849–874. <https://doi.org/10.1037/a0019842>
- Kinouchi, O., & Copelli, M. (2006). Optimal dynamical range of excitable networks at criticality. *Nature Physics*, 2(5), 348–351. <https://doi.org/10.1038/nphys289>
- Koch, I., Poljac, E., Müller, H., & Kiesel, A. (2018). Cognitive structure, flexibility, and plasticity in human multitasking—An integrative review of dual-task and task-switching research. *Psychological Bulletin*, 144(6), 557–583. <https://doi.org/10.1037/bul0000144>
- Kolvoort, I. R., Wainio-Theberge, S., Wolff, A., & Northoff, G. (2020). Temporal integration as “common currency” of brain and self-scale-free activity in resting-state EEG correlates with temporal delay effects on self-relatedness. *Human Brain Mapping*, 41(15), 4355–4374. <https://doi.org/10.1002/hbm.25129>
- Lei, X., Wang, Y., Yuan, H., & Chen, A. (2015). Brain scale-free properties in awake rest and NREM sleep: A simultaneous EEG/fMRI study. *Brain Topography*, 28(2), 292–304. <https://doi.org/10.1007/s10548-014-0399-x>
- Lendner, J. D., Helfrich, R. F., Mander, B. A., Romundstad, L., Lin, J. J., Walker, M. P., Larsson, P. G., & Knight, R. T. (2020). An electrophysiological marker of arousal level in humans. *eLife*, 9, e55092. <https://doi.org/10.7554/eLife.55092>
- Liang, J., & Zhou, C. (2022). Criticality enhances the multilevel reliability of stimulus responses in cortical neural networks. *PLoS Computational Biology*, 18(1), e1009848. <https://doi.org/10.1371/journal.pcbi.1009848>
- Lindén, H., Pettersen, K. H., & Einevoll, G. T. (2010). Intrinsic dendritic filtering gives low-pass power spectra of local field potentials. *Journal of Computational Neuroscience*, 29(3), 423–444. <https://doi.org/10.1007/s10827-010-0245-4>
- Little, T. D., Lindenberger, U., & Nesselroade, J. R. (1999). On selecting indicators for multivariate measurement and modeling with latent variables: When “good” indicators are bad and “bad” indicators are good. *Psychological Methods*, 4(2), 192–211. <https://doi.org/10.1037/1082-989X.4.2.192>
- Ma, L., Chang, L., Chen, X., & Zhou, R. (2017). Working memory test battery for young adults: Computerized working memory assessment. *PLoS One*, 12(3), e0175047. <https://doi.org/10.1371/journal.pone.0175047>
- McSweeney, M., Morales, S., Valadez, E. A., Buzzell, G. A., & Fox, N. A. (2021). Longitudinal age- and sex-related change in background aperiodic activity during early adolescence. *Developmental Cognitive Neuroscience*, 52, 101035. <https://doi.org/10.1016/j.dcn.2021.101035>
- Merkin, A., Sghirripa, S., Graetz, L., Smith, A. E., Hordacre, B., Harris, R., Pitcher, J., Semmler, J., Rogasch, N. C., & Goldworthy, M. (2023). Do age-related differences in aperiodic neural activity explain differences in resting EEG alpha? *Neurobiology of Aging*, 121, 78–87. <https://doi.org/10.1016/j.neurobiolaging.2022.09.003>
- Miller, E. K., & Wallis, J. D. (2009). Executive function and higher-order cognition: Definition and neural substrates. In L. R. Squire (Ed.), *Encyclopedia of neuroscience* (pp. 99–104). Academic Press.
- Miller, K. J., Sorensen, L. B., Ojemann, J. G., & den Nijs, M. (2009). Power-law scaling in the brain surface electric potential. *PLoS Computational Biology*, 5(12), e1000609. <https://doi.org/10.1371/journal.pcbi.1000609>
- Milli, S., Lieder, F., & Griffiths, T. L. (2021). A rational reinterpretation of dual-process theories. *Cognition*, 217, 104881. <https://doi.org/10.1016/j.cognition.2021.104881>
- Miyake, A., Friedman, N. P., Emerson, M. J., Witzki, A. H., Howerter, A., & Wager, T. D. (2000). The unity and diversity of executive functions and their contributions to complex “frontal lobe” tasks: A latent variable analysis. *Cognitive Psychology*, 41(1), 49–100. <https://doi.org/10.1006/cogp.1999.0734>
- Nelson, C. A., de Haan, M., & Thomas, K. M. (2015). The development of higher cognitive (executive) functions. In C. A. Nelson, M. de Haan & K. M. Thomas (Eds.), *Neuroscience of cognitive development: The role of experience and the developing brain* (pp. 143–153). John Wiley & Sons, Inc. <https://doi.org/10.1002/9780470939413.ch10>
- Ostlund, B. D., Alperin, B. R., Drew, T., & Karalunas, S. L. (2021). Behavioral and cognitive correlates of the aperiodic (1/f-like) exponent of the EEG power spectrum in adolescents with and without ADHD. *Developmental Cognitive Neuroscience*, 48, 100931. <https://doi.org/10.1016/j.dcn.2021.100931>
- Ouyang, G., Hildebrandt, A., Schmitz, F., & Herrmann, C. S. (2020). Decomposing alpha and 1/f brain activities reveals their differential associations with cognitive processing speed. *NeuroImage*, 205, 116304. <https://doi.org/10.1016/j.neuroimage.2019.116304>
- Penke, L., Maniega, S. M., Bastin, M. E., Valdés Hernández, M. C., Murray, C., Royle, N. A., Starr, J. M., Wardlaw, J. M., & Deary, I. J. (2012). Brain white matter tract integrity as a neural foundation for general intelligence. *Molecular Psychiatry*, 17(10), 1026–1030. <https://doi.org/10.1038/mp.2012.66>
- Pereda, E., Gamundi, A., Rial, R., & González, J. (1998). Non-linear behaviour of human EEG: Fractal exponent versus correlation dimension in awake and sleep stages. *Neuroscience Letters*, 250(2), 91–94. [https://doi.org/10.1016/S0304-3940\(98\)00435-2](https://doi.org/10.1016/S0304-3940(98)00435-2)
- Pivik, R. T., Broughton, R. J., Coppola, R., Davidson, R. J., Fox, N., & Nuwer, M. R. (1993). Guidelines for the recording and quantitative analysis of electroencephalographic activity in research contexts. *Psychophysiology*, 30(6), 547–558. <https://doi.org/10.1111/j.1469-8986.1993.tb02081.x>
- R Development Core Team. (2010). *R: A language and environment for statistical computing*. R Foundation for Statistical Computing. <http://www.R-project.org>
- Schmiedek, F., Oberauer, K., Wilhelm, O., Süß, H.-M., & Wittmann, W. W. (2007). Individual differences in components of reaction time distributions and their relations to working memory and intelligence. *Journal of Experimental Psychology: General*, 136(3), 414–429. <https://doi.org/10.1037/0096-3445.136.3.414>
- Schneider, W., & Chein, J. M. (2003). Controlled & automatic processing: Behavior, theory, and biological mechanisms. *Cognitive Science*, 27(3), 525–559. [https://doi.org/10.1016/S0364-0213\(03\)00011-9](https://doi.org/10.1016/S0364-0213(03)00011-9)
- Schneider, W., & Shiffrin, R. M. (1977). Controlled and automatic human information processing: I. Detection, search, and attention. *Psychological Review*, 84(1), 1–66. <https://doi.org/10.1037/0033-295X.84.1.1>
- Shew, W. L., & Plenz, D. (2012). The functional benefits of criticality in the cortex. *The Neuroscientist*, 19(1), 88–100. <https://doi.org/10.1177/1073858412445487>
- Steyvers, M., Hawkins, G. E., Karayanidis, F., & Brown, S. D. (2019). A large-scale analysis of task switching practice effects across the lifespan. *Proceedings of the National Academy of Sciences of the United States of America*, 116(36), 17735–17740. <https://doi.org/10.1073/pnas.1906788116>
- Supekar, K., Swigart, A. G., Tenison, C., Jolles, D. D., Rosenberg-Lee, M., Fuchs, L., & Menon, V. (2013). Neural predictors of

- individual differences in response to math tutoring in primary-grade school children. *Proceedings of the National Academy of Sciences of the United States of America*, 110(20), 8230–8235. <https://doi.org/10.1073/pnas.1222154110>
- Thuwal, K., Banerjee, A., & Roy, D. (2021). Aperiodic and periodic components of ongoing oscillatory brain dynamics link distinct functional aspects of cognition across adult lifespan. *eNeuro*, 8(5), ENEURO.0224-21.2021. <https://doi.org/10.1523/ENEURO.0224-21.2021>
- Voytek, B., Kramer, M. A., Case, J., Lepage, K. Q., Tempesta, Z. R., Knight, R. T., & Gazzaley, A. (2015). Age-related changes in $1/f$ neural electrophysiological noise. *The Journal of Neuroscience*, 35(38), 13257–13265. <https://doi.org/10.1523/jneurosci.2332-14.2015>
- Waschke, L., Donoghue, T., Fiedler, L., Smith, S., Garrett, D. D., Voytek, B., & Obleser, J. (2021). Modality-specific tracking of attention and sensory statistics in the human electrophysiological spectral exponent. *eLife*, 10, e70068. <https://doi.org/10.7554/eLife.70068>
- Weber, J., Klein, T., & Abeln, V. (2020). Shifts in broadband power and alpha peak frequency observed during long-term isolation. *Scientific Reports*, 10(1), 17987. <https://doi.org/10.1038/s41598-020-75127-0>
- Wen, H., & Liu, Z. (2016). Separating fractal and oscillatory components in the power Spectrum of neurophysiological signal. *Brain Topography*, 29(1), 13–26. <https://doi.org/10.1007/s10548-015-0448-0>
- Winkler, I., Haufe, S., & Tangermann, M. (2011). Automatic classification of artifactual ICA-components for artifact removal in EEG signals. *Behavioral and Brain Functions*, 7(1), 30. <https://doi.org/10.1186/1744-9081-7-30>
- Yves, R. (2012). lavaan: An R package for structural equation modeling. *Journal of Statistical Software*, 48(2), 1–36. <https://doi.org/10.18637/jss.v048.i02>
- Zhang, S., Yan, X., Wang, Y., Liu, B., & Gao, X. (2021). Modulation of brain states on fractal and oscillatory power of EEG in brain-computer interfaces. *Journal of Neural Engineering*, 18(5), 056047. <https://doi.org/10.1088/1741-2552/ac2628>
- Zimmern, V. (2020). Why brain criticality is clinically relevant: A scoping review. *Frontiers in Neural Circuits*, 14, 54. <https://doi.org/10.3389/fncir.2020.00054>

How to cite this article: Pei, L., Zhou, X., Leung, F. K. S., & Ouyang, G. (2023). Differential associations between scale-free neural dynamics and different levels of cognitive ability. *Psychophysiology*, 60, e14259. <https://doi.org/10.1111/psyp.14259>